Catalysis Today 138 (2008) 249–252

Contents lists available at ScienceDirect

Catalysis Today

journal homepage: www.elsevier.com/locate/cattod

# Thermodynamics of hydrogen adsorption on the zeolite Ca-Y

G. Turnes Palomino *, M.R. Llop Carayol, C. Otero Areán

*Department of Chemistry, University of the Balearic Islands, 07122 Palma de Mallorca, Spain*

ARTICLE INFO

*Article history:*
Available online 7 July 2008

*Keywords:*
Hydrogen adsorption
Hydrogen storage
Adsorption enthalpy
Infrared spectroscopy
Porous materials
Zeolites

ABSTRACT

Variable-temperature infrared spectroscopy was used for a thermodynamic study on hydrogen adsorption on the zeolite Ca-Y. Adsorption renders the H–H stretching mode infrared active, at 4078 $cm^{-1}$; and simultaneous measurement of IR absorbance and hydrogen equilibrium pressure, over a range of temperature, allowed standard adsorption enthalpy and entropy to be determined. They resulted to be $\Delta H^\circ = -15.0(\pm1.0)$ kJ $mol^{-1}$ and $\Delta S^\circ = -127(\pm10)$ J $mol^{-1}$ $K^{-1}$, respectively. These relatively high values of adsorption enthalpy and entropy are discussed in the broader context of corresponding data for other hydrogen adsorbents.

## 1. Introduction

Hydrogen storage and transport constitutes a key enabling technology for the advent of a hydrogen-based energy transition [1–3]. Means for safe and cost effective hydrogen storage are needed for both, stationary applications (*e.g.* for heating and air conditioning of buildings) and for the transportation sector. However, because of technical considerations regarding mass and volume (and also heat management), the use of hydrogen for propulsion of road vehicles posses the most demanding challenges [4–6]. Currently, a large effort is being made worldwide in the attempt to develop functional materials for on-board hydrogen storage and delivery. Most of these materials belong to two distinct groups; they either show hydrogen chemisorption usually followed by compound formation or they reversibly adsorb molecular hydrogen. The first group is typified by metal hydrides [7–12]; the second group (constituted by highly porous solids) includes active carbons [13–18], metal-organic frameworks (MOFs) [18–23] and other hydrogen adsorbents such as porous organic polymers and zeolites [23–26]. Physisorption on porous solids has the advantage (over metal hydrides) of fast hydrogen uptake and release kinetics. However, a significant hurdle of hydrogen storage using physisorption is that the interaction between adsorbed hydrogen molecules and the pore walls of most porous adsorbents is by weak van der Waals forces, giving rise to an interaction energy of the order of only −5 to −6 kJ $mol^{-1}$. It should be noted that for an optimum storage-delivery cycle the adsorption enthalpy ($\Delta H^\circ$) should be neither too low (so as to enhance storage) nor to high (to facilitate release). Following this consideration, an optimum value of $\Delta H^\circ = -15$ kJ $mol^{-1}$ has recently been proposed [27]. Most of the reported values of standard adsorption enthalpy of hydrogen on zeolites go from about −5 to −11 kJ $mol^{-1}$; the smallest of these values corresponding to alkali-metal-exchanged ferrierite [28,29], and the largest to protonic chabazite [30] and to sodium-exchanged zeolites and related materials of the type ZSM-5, FAU and ETS-10 [31–35]. Note that these hydrogen adsorbents contain only monovalent (extra-framework) cations or protons. However, very recently, some reports have shown that by using MOFs [36,37] or zeolites [38,39] having exposed (coordinatively unsaturated) divalent metal ions, *e.g.* Ni(II) [36], Mn(II) [37] or Mg(II) [38,39], a hydrogen adsorption enthalpy in the range of −10 to −18 kJ $mol^{-1}$ can be obtained. Following these promising developments, and with the aim of gaining further knowledge on the potential shown by porous adsorbents incorporating divalent metal cations, we report on a thermodynamic study of hydrogen adsorption (at a low temperature) on the faujasite-type zeolite Ca-Y. Both, standard adsorption enthalpy and entropy were experimentally determined by means of variable-temperature IR spectroscopy, and the role of entropy change is highlighted.

## 2. Materials and methods

The Y-zeolite sample used (Si:Al = 2.4) was synthesized in its sodium form by following standard procedures [40] and it was then repeatedly exchanged with a 0.5 M solution of calcium

---

* Corresponding author. Tel.: +34 971173250; fax: +34 971173426.
*E-mail address:* g.turnes@uib.es (G. Turnes Palomino).

0920-5861/$ – see front matter © 2008 Elsevier B.V. All rights reserved.
doi:10.1016/j.cattod.2008.05.021

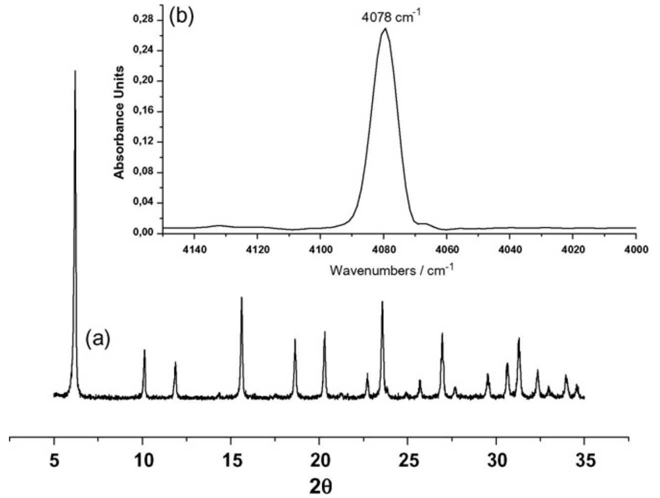

**Fig. 1.** (a) X-ray diffractogram (Cu Kα radiation) of Ca-Y. (b) IR spectrum of hydrogen adsorbed on Ca-Y, at 77 K and 1 mbar; the blank zeolite spectrum was subtracted.

nitrate. Powder X-ray diffraction of the exchanged sample showed good crystallinity, as seen in Fig. 1a, and all diffraction lines could be assigned to the expected faujasite-type structure [41]. After hydrogen adsorption at 77 K (see below) the IR spectrum in the H–H stretching region gave a single absorption band at 4078 $\mathrm{cm^{-1}}$. On account of its large bathochromic shift from the gas phase value of 4163 $\mathrm{cm^{-1}}$, this band is assigned to hydrogen adsorbed on $\mathrm{Ca^{2+}}$ ions. No IR absorption bands were observed in the range of 4090–4150 $\mathrm{cm^{-1}}$, where usually appear the signals corresponding to hydrogen interacting with $\mathrm{Na^{+}}$ ions [42,43]. This fact confirms total ion exchange of calcium for sodium. Note that a partial exchange of protons for sodium would give an O–H stretching band in the range of 3550–3650 $\mathrm{cm^{-1}}$ [44], which was not observed in the infrared spectra.

For IR spectroscopy, a thin self-supported wafer of the Ca-Y sample was prepared and activated (outgassed) in a dynamic vacuum (residual pressure $< 10^{-4}$ mbar) for 3 h at 700 K inside a home-made IR cell, described elsewhere [45,46], which allowed in situ sample activation, gas dosage and variable temperature IR spectroscopy to be carried out. After recording the blank spectrum of the zeolite wafer at liquid nitrogen temperature the cell was dosed with hydrogen, it was then closed and spectra were taken at several fixed temperatures, while simultaneously registering temperature and hydrogen equilibrium pressure inside the cell. For that purpose, the cell was equipped with a platinum resistance thermometer (Tinsley) and a capacitance pressure gauge (Baratron). The precision of these measurements was about ±2 K and $\pm 2 \times 10^{-2}$ mbar, respectively. Transmission IR spectra were recorded, at 3 $\mathrm{cm^{-1}}$ resolution, by using a Bruker IFS66 instrument.

A set of IR spectra taken over a temperature range while simultaneously measuring infrared absorbance, $A$, temperature, $T$, and hydrogen equilibrium pressure, $p$, inside the closed IR cell can be used to derive standard adsorption enthalpy ($\Delta H^\circ$) and entropy ($\Delta S^\circ$) by following the variable-temperature infrared (VTIR) spectroscopic method described in detail elsewhere [47]. Briefly, at any given temperature, the integrated intensity of the characteristic IR absorption band should be proportional to surface coverage, $\theta$, thus giving information on the activity (in the thermodynamic sense) of both the adsorbed species and the empty adsorbing sites; simultaneously, the equilibrium pressure does the same for the gas phase. Hence, the corresponding adsorption equilibrium constant, $k$, can be determined, and the variation of $k$ with temperature leads to the corresponding values of adsorption enthalpy and entropy. For deriving these values, integrated band intensity, temperature, and hydrogen equilibrium pressure were considered to be interrelated by the (Langmuir-type) Eq. (1) below:

$$\theta = \frac{A}{A_\mathrm{M}} = \frac{k(T)\,p}{1 + k(T)\,p} \tag{1}$$

where $A_\mathrm{M}$ stands for the integrated absorbance corresponding to full coverage. Eq. (1) can be combined with the well-known van't Hoff Eq. (2) to yield Eq. (3) below:

$$k(T) = \exp\left(\frac{-\Delta H^\circ}{RT}\right)\exp\left(\frac{\Delta S^\circ}{R}\right) \tag{2}$$

$$\ln\left[\frac{A}{(A_\mathrm{M} - A)\,p}\right] = \left(\frac{-\Delta H^\circ}{RT}\right) + \left(\frac{\Delta S^\circ}{R}\right) \tag{3}$$

from which $\Delta H^\circ$ and $\Delta S^\circ$ can be derived. It should be noted, however, that knowledge of $A_\mathrm{M}$ is needed. An approximate value of this parameter was obtained by recording IR spectra for increasing doses of hydrogen at 77 K, and extrapolating the resulting Langmuir isotherm. This approximate value was then refined by plotting the left-hand side of Eq. (3) against reciprocal temperature for $A_\mathrm{M}$ values which were changed in steps of $\pm 0.05\ \mathrm{cm^{-1}}$ around the original value, and selecting (by linear regression) the best fit to the whole set of experimental data.

## 3. Results and discussion

Infrared spectra of molecular hydrogen adsorbed, at a low temperature, on alkali-metal exchanged faujasites (X and Y), mordenites, ferrierites and ZSM-5 zeolites were reported by several authors [28,29,31,33,42,43]. These spectra show a main IR absorption band in the 4090–4150 $\mathrm{cm^{-1}}$ range, which corresponds to the fundamental H–H stretching mode of the adsorbed molecule. Perturbation of adsorbed hydrogen (mainly) by the cationic adsorption centre renders this vibrational mode IR active and brings about a bathochromic shift from the gas phase value of 4163 $\mathrm{cm^{-1}}$, which corresponds to the Raman active H–H stretching mode of free molecule. This bathochromic shift usually correlates with the cation polarizing power, which is in agreement with theoretical calculations [48] showing that $\mathrm{H_2}$ interaction with alkali-metal cations is dominated by the polarization contribution. Thus, for hydrogen adsorbed on Li-ZSM-5, Na-ZSM-5 and K-ZSM-5 the characteristic IR absorption band appears at 4092 ($\Delta\upsilon = -71\ \mathrm{cm^{-1}}$), 4101 ($\Delta\upsilon = -62\ \mathrm{cm^{-1}}$) and 4112 $\mathrm{cm^{-1}}$ ($\Delta\upsilon = -51\ \mathrm{cm^{-1}}$), respectively [31,32]. For a faujasite-type zeolite partially exchanged with $\mathrm{Mg^{2+}}$, (Mg,Na)-Y, the IR absorption band corresponding to $\mathrm{H_2}$ interacting with magnesium ions was observed at 4056 $\mathrm{cm^{-1}}$ ($\Delta\upsilon = -106\ \mathrm{cm^{-1}}$) [38,39]; the much larger bathochromic shift correlates with the higher polarizing power of $\mathrm{Mg^{2+}}$ (as compared to that of alkali-metal cations). According to this trend, hydrogen adsorbed on Ca-Y gives the characteristic IR absorption band at 4078 $\mathrm{cm^{-1}}$ ($\Delta\upsilon = -85\ \mathrm{cm^{-1}}$), as seen in Fig. 1b.

Representative variable temperature FT-IR spectra (in the H–H stretching region) of $\mathrm{H_2}$ adsorbed on Ca-Y are depicted in Fig. 2; they were obtained, for a fixed dose of hydrogen, over a temperature range going from 101 to 124 K. From the whole set of spectra recorded (not all of them shown in Fig. 2), a linear plot of the left-hand side of Eq. (3) against reciprocal temperature was obtained, as shown in Fig. 3. From this plot, the standard enthalpy of adsorption resulted to be $\Delta H^\circ = -15.0\ \mathrm{kJ\ mol^{-1}}$. The corresponding entropy change is $\Delta S^\circ = -127\ \mathrm{J\ mol^{-1}\ K^{-1}}$. The estimated error limits are $\pm 1\ \mathrm{kJ\ mol^{-1}}$ for enthalpy and $\pm 10\ \mathrm{J\ mol^{-1}\ K^{-1}}$ for entropy.

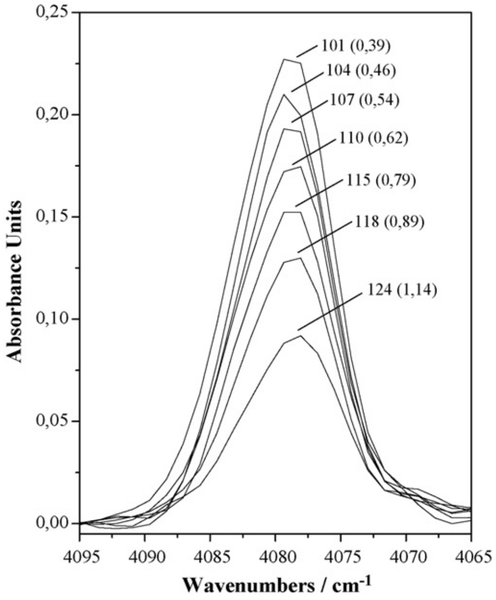

**Fig. 2.** Representative variable-temperature FT-IR spectra (zeolite blank subtracted) in the H–H stretching region of hydrogen adsorbed on Ca-Y. Temperature, in K, and pressure (mbar, in brackets) as shown.

The same (VTIR) method used here was also applied for determining standard enthalpy and entropy changes involved in hydrogen adsorption on other cation-exchanged zeolites. In order to facilitate discussion in a broader context, Table 1 summarizes available data. Two main points are worth of notice: (i) in general terms, adsorption enthalpy correlates with cation polarizing power and (ii) within the established error limits, adsorption entropy appears to correlate with adsorption enthalpy (for all cases where both, $\Delta H^\circ$ and $\Delta S^\circ$ data are available). It should also be borne in mind that thermodynamic data reported in Table 1 correspond to localized hydrogen adsorption on the zeolite (cationic) adsorbing centres (*i.e.* up to monolayer coverage). Once these centres are saturated, delocalized (multilayer) hydrogen adsorption would, presumably, lead to a smaller value of gas–solid interaction energy. However, since non-polarized hydrogen molecules do not give an IR signal, corresponding thermodynamic data cannot be obtained by using the VTIR method.

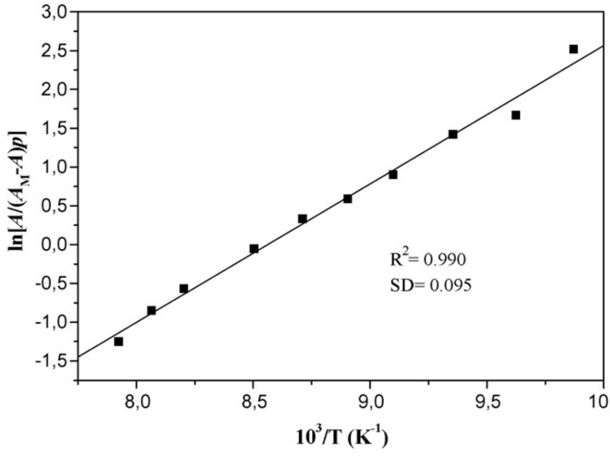

**Fig. 3.** Plot of the left-hand side of Eq. (3) against reciprocal temperature. *R*, linear regression coefficient and S.D., standard deviation.

**Table 1**
Standard enthalpy, $\Delta H^\circ$, and entropy, $\Delta S^\circ$, of hydrogen adsorption on basic zeolites

| Zeolite | $\Delta H^\circ$ (kJ mol$^{-1}$) ($\pm 1$) | $\Delta S^\circ$ (J mol$^{-1}$ K$^{-1}$) ($\pm 10$) | Reference |
|---|---|---|---|
| Li-FER | −4.1 | −57 | [19] |
| Na-FER | −6.0 | −78 | [18] |
| K-FER | −3.5 | −57 | [18] |
| Li-ZSM-5 | −6.5 | −90 | [22] |
| Na-ZSM-5 | −10.3 | −121 | [21,22] |
| | −11.0 | – | [33] |
| (Na,K)-ETS-10 | −8.7 | – | [34] |
| (H,Na)-Y | −11.4 | – | [35] |
| H-CHA | −9.7 | – | [30] |
| (Na,Mg)-Y | −18.2 | −136 | [25,26] |
| Ca-Y | −15 | −127 | This work |

For localized adsorption, correlation between adsorption enthalpy and cation polarizing power is reflected in the data shown in Table 1. As a general rule, $\Delta H^\circ$ tends to show a larger (absolute) value when the polarizing power of the cation increases and, as expected, the zeolite containing $Mg^{2+}$ (the strongest polarizing cation) shows the largest $\Delta H^\circ$ value. However, there are exceptions to this rule that testify to the role of the nearby zeolite framework; thus, hydrogen adsorption on Li-exchanged zeolites involves a smaller enthalpy change than adsorption on the corresponding Na-exchanged zeolites. Recent calculations, at the periodic DFT level, for hydrogen adsorption on Li-FER and Na-FER [29,49] have shown that (because of the small size of the $Li^+$ ion) residual interactions of the adsorbed hydrogen molecule with the zeolite framework (for Li-FER) result in a slight destabilization of the corresponding adsorption complex.

Data summarized in Table 1 strongly suggest that there is a positive correlation between adsorption enthalpy and entropy; in general terms, higher (absolute) values of $\Delta H^\circ$ correspond to higher values of $\Delta S^\circ$. A positive correlation, also termed entropy–enthalpy compensation [50,51], was also reported by several authors for a wide range of chemical processes driven by weak interaction forces, including hydrogen bonding [52], Langmuir-type adsorption from solution [53] and formation of weakly associated (van der Waals) molecular complexes [51,54]. For the case of hydrogen adsorption on zeolites, the observed enthalpy–entropy correlation (Table 1) is likely to arise because of a stronger (enthalpy related) interaction between hydrogen molecules and zeolite adsorbing centres leads to a larger decrease of motion freedom, and hence to (entropy related) greater order of the system.

Zeolites themselves are not likely candidates for on-board hydrogen storage systems (*e.g.*, for propulsion of road vehicles), because the relatively high density of the aluminosilicate framework necessarily leads to a low storage capacity [23,55]. However, model studies on zeolites do have the potential to facilitate insight relevant to lighter porous adsorbents (*e.g.*, MOFs containing low-coordinated metal cations), as briefly considered below.

Optimum thermodynamic requirements for hydrogen storage by physisorption were discussed by Bhatia and Myers [27] with a focus on porous carbons. Assuming Langmuir-type adsorption and following standard thermodynamics, they derived Eq. (4) below:

$$\Delta H^\circ_{\mathrm{opt}} = T\,\Delta S^\circ + \left[\left(\frac{RT}{2}\right)\ln\left(\frac{P_1 P_2}{P_0^2}\right)\right] \qquad (4)$$

which gives the optimum value of adsorption enthalpy ($\Delta H^\circ_{\mathrm{opt}}$) for maximum hydrogen storage and delivery as a function of temperature ($T$) and adsorption entropy ($\Delta S^\circ$), being $P_0$ the standard pressure to which $\Delta S^\circ$ is referred (usually taken to be 1 bar), $P_1$ the hydrogen loading pressure and $P_2$ the exhaust delivery pressure.

For carbons, which show only weak (dispersion-type) interaction with adsorbed hydrogen, $\Delta S^\circ$ was calculated to be $-66.5$ J mol$^{-1}$ K$^{-1}$ [27]. Assuming $P_1 = 30$ bar and $P_2 = 1.5$ bar as being reasonable pressure values for the hydrogen storage-delivery cycle, the above value of $\Delta S^\circ$ gives, when inserted in Eq. (4), an optimum enthalpy change of $\Delta H^\circ_{\mathrm{opt}} = -15.1$ kJ mol$^{-1}$ for operation at ambient temperature (298 K). However, because of the enthalpy–entropy correlation discussed above, adsorbents showing relatively high $\Delta H^\circ$ values would be expected to show a correspondingly larger entropy change; which would have to be taken into account when applying Eq. (4). In this context, it is relevant to point out that MOFs having coordinatively unsaturated metal cations constitute a case similar to that of cation-exchanged zeolites, as testified by recent reports [37,56–59] giving $\Delta H^\circ$ values of about $-10$ kJ mol$^{-1}$ for hydrogen adsorbed on MOFs containing exposed Mg(II), Mn(II) and Zn(II) cationic adsorbing centres. This adsorption enthalpy is significantly higher than that of $-5.8$ kJ mol$^{-1}$ typical of hydrogen on carbons [23], thus showing that the role played by polarization of the adsorbed dihydrogen molecule applies not only to zeolites, but also to other porous hydrogen adsorbents containing coordinatively unsaturated metal cations.

Finally, we remark that $\Delta S^\circ$ values reported in Table 1 are referred to a standard pressure of 1 Torr (1.33 mbar) representative of the pressure range at which IR spectra were obtained. Within the perfect gas approximation, an amount of +55 J mol$^{-1}$ K$^{-1}$ has to be added to $\Delta S^\circ$ values reported in Table 1 in order to have corresponding values referred to a standard pressure $P_0 = 1$ bar (*e.g.*, the corresponding value for Ca-Y is $-72$ J mol$^{-1}$ K$^{-1}$). Note that this change of reference state has no effect on standard adsorption enthalpy.

## 4. Conclusions

Thermodynamics of hydrogen adsorption on the faujasite-type zeolite Ca-Y was studied by using variable temperature IR spectroscopy. The standard adsorption enthalpy (at a low coverage) was found to be $\Delta H^\circ = -15.0$ kJ mol$^{-1}$, which is significantly larger than that shown by alkali-metal exchanged zeolites, but smaller (in absolute value) than that of Mg-exchanged zeolite-Y. Differences were explained in terms of relative polarizing power of the cations involved. Hydrogen adsorption entropy ($\Delta S^\circ$), which was also experimentally determined, was compared with corresponding values for other alkaline zeolites. This comparison showed that a positive correlation occurs between $\Delta H^\circ$ and $\Delta S^\circ$; *i.e.*, $\Delta S^\circ$ was found to take a larger value the larger is the corresponding enthalpy change. Possible implications for hydrogen storage by physisorption on porous solids were briefly discussed.

## Acknowledgements

Financial support from the Spanish MEC and FEDER funds (Project MAT2005-05350) and from the Conselleria d'Economia, Hisenda e Innovació de les Illes Balears (Project PROGECIB-22A) is gratefully acknowledged.

## References

[1] A.A. Strub, G. Imarisio, Hydrogen as an Energy Vector, D. Reidel, Dordrecht, 1980.
[2] D. Sperling, J.S. Cannon (Eds.), The Hydrogen Energy Transition, Elsevier, Amsterdam, 2004.
[3] R. Coontz, B. Hanson, Science 305 (2004) 957.
[4] R.M. Dell, D.A.J. Rand, J. Power Sources 100 (2001) 2.
[5] R. von Helmolt, U. Eberle, J. Power Sources 165 (2007) 833.
[6] IEA Hydrogen co-ordination group, Hydrogen production and storage: R&D priorities and gaps, OECD/IEA, 2006.
[7] L. Schlapbach, A. Züttel, Nature 414 (2001) 353.
[8] A. Zuttel, Mater. Today (2003) 24.
[9] W. Grochala, P.P. Edwards, Chem. Rev. 104 (2004) 1283.
[10] M. Bououdina, D. Grant, G. Walker, Int. J. Hydrogen Energy 31 (2006) 177.
[11] S. Satyapal, J. Petrovic, C. Read, G. Thomas, G. Ordaz, Catal. Today 120 (2007) 246.
[12] F. Schüth, B. Bogdanovich, M. Felderhoff, Chem. Commun. (2004) 2249.
[13] R. Ströbel, J. Garche, P.T. Moseley, L. Jörissen, G. Wolf, J. Power Sources 159 (2006) 781.
[14] Z. Yang, Y. Xia, R. Mokaya, J. Am. Chem. Soc. 129 (2007) 1673.
[15] M. Felderhoff, C. Weidenthaler, R. von Helmolt, U. Eberle, Phys. Chem. Chem. Phys. 9 (2007) 2643.
[16] M. Armandi, B. Bonelli, C. Otero Areán, E. Garrone, Micropor. Mesopor. Mater. 112 (2008) 411.
[17] P. Kowalczyk, R. Holyst, M. Terrones, H. Terrones, Phys. Chem. Chem. Phys. 9 (2007) 1786.
[18] K.M. Thomas, Catal. Today 120 (2007) 389.
[19] D.J. Collins, H.C. Zhou, J. Mater. Chem. 17 (2007) 3154.
[20] J.L.C. Rowsell, O.M. Yaghi, Angew. Chem. Int. Ed. 44 (2005) 4670.
[21] O.K. Farha, A.M. Spokoyny, K.L. Mulfort, F. Frederick Hawthorne, C.A. Mirkin, J.T. Huup, J. Am. Chem. Soc. 129 (2007) 12680.
[22] A.J. Fletcher, K.M. Thomas, M.J. Rosseinsky, J. Solid State Chem. 178 (2005) 2491.
[23] A.W.C. van der Berg, C. Otero Areán, Chem. Commun. (2008) 668.
[24] P.M. Budd, A. Butler, J. Selbie, K. Mahmood, N.B. McKeown, B. Ghanem, K. Msayib, D. Book, A. Walton, Phys. Chem. Chem. Phys. 9 (2007) 1802.
[25] B.S. Ghanem, K.J. Msayib, N.B. McKeown, K.D.M. Harris, Z. Pan, P.M. Budd, A. Butler, J. Selbie, D. Book, A. Walton, Chem. Commun. (2007) 67.
[26] J. Germain, J.M.J. Fréchet, F. Svec, J. Mater. Chem. 17 (2007) 4989.
[27] S.K. Bhatia, A.L. Myers, Langmuir 22 (2006) 1688.
[28] C. Otero Areán, G. Turnes Palomino, E. Garrone, D. Nachtigallová, P. Nachtigall, J. Phys. Chem. B 110 (2006) 395.
[29] P. Nachtigall, E. Garrone, G. Turnes Palomino, M. Rodríguez Delgado, D. Nachtigallová, C. Otero Areán, Phys. Chem. Chem. Phys. 8 (2006) 2286.
[30] A. Zecchina, S. Bordiga, J.G. Vitillo, G. Ricchiardi, C. Lamberti, G. Spoto, M. Bjørgen, K.P. Lillerud, J. Am. Chem. Soc. 127 (2005) 6361.
[31] C. Otero Areán, M. Rodríguez Delgado, G. Turnes Palomino, M. Tomás Rubio, N.M. Tsyganenko, A.A. Tsyganenko, E. Garrone, Micropor. Mesopor. Mater. 80 (2005) 247.
[32] G. Turnes Palomino, M. Rodríguez Delgado, N.M. Tsyganenko, A.A. Tsyganenko, E. Garrone, B. Bonelli, O.V. Manoilova, C. Otero Areán, Stud. Surf. Sci. Catal. 158 (2005) 853.
[33] G. Spoto, E. Gribov, S. Bordiga, C. Lamberti, G. Ricchiardi, D. Scarano, A. Zecchina, Chem. Commun. (2004) 2768.
[34] G. Ricchiardi, J.G. Vitillo, D. Cocina, E.N. Gribov, A. Zecchina, Phys. Chem. Chem. Phys. 9 (2007) 2753.
[35] E.N. Gribov, D. Cocina, G. Spoto, S. Bordiga, G. Ricchiardi, A. Zecchina, Phys. Chem. Chem. Phys. 8 (2006) 1186.
[36] P.M. Forster, J. Eckert, B.D. Heiken, J.B. Parise, J.W. Yoon, S.H. Jhung, J.S. Chang, A.K. Cheetham, J. Am. Chem. Soc. 128 (2006) 16846.
[37] M. Dinca, A. Dailly, Y. Liu, C.M. Brown, D.A. Neumann, J.R. Long, J. Am. Chem. Soc. 128 (2006) 16876.
[38] G. Turnes Palomino, M.R. Llop Carayol, C. Otero Areán, J. Mater. Chem. 16 (2006) 2884.
[39] C. Otero Areán, G. Turnes Palomino, M.R. Llop Carayol, Appl. Surf. Sci. 253 (2007) 5701.
[40] R.M. Szostak, Molecular Sieves, Van Nostrand Reinhold, 1989.
[41] M.M.J. Treacy, J.B. Higgins, Collection of Simulated XRD Powder Patterns for Zeolites, Elsevier, 2001.
[42] L.M. Kustov, V.B. Kazansky, J. Chem. Soc., Faraday Trans. 87 (1991) 2675.
[43] V.B. Kazansky, J. Mol. Catal. A 141 (1999) 83.
[44] A. Zecchina, C. Otero Areán, Chem. Soc. Rev. 25 (1996) 187.
[45] A.A. Tsyganenko, P. Yu Storozhev, C. Otero Areán, Kinet. Catal. 45 (2004) 530.
[46] C. Otero Areán, O.V. Manoilova, A.A. Tsyganenko, G. Turnes Palomino, M. Peñarroya Mentruit, F. Geobaldo, E. Garrone, Eur. J. Inorg. Chem. (2001) 1739.
[47] E. Garrone, C. Otero Areán, Chem. Soc. Rev. 34 (2005) 846.
[48] X. Solans-Monfort, V. Branchadell, M. Sodupe, C.M. Zicovich-Wilson, E. Gribov, G. Spoto, C. Busco, P. Ugliengo, J. Phys. Chem. B 108 (2004) 2878.
[49] C. Otero Areán, D. Nachtigallová, P. Nachtigall, E. Garrone, M. Rodríguez Delgado, Phys. Chem. Chem. Phys. 9 (2007) 1421.
[50] A.K. Galwey, Adv. Catal. 26 (1977) 247.
[51] L. Liu, Q.X. Guo, Chem. Rev. 101 (2001) 673.
[52] D.H. Williams, E. Stephens, D.P. O'Brien, M. Zhou, Angew. Chem. Int. Ed. 43 (2004) 6596.
[53] G. Sugihara, D.S. Shigematsu, S. Nagadome, S. Lee, Y. Sasaki, H. Igimi, Langmuir 16 (2000) 1825.
[54] M.S. Westwell, M.S. Searle, J. Klein, D.H. Williams, J. Phys. Chem. 100 (1996) 16000.
[55] J.G. Vitillo, G. Ricchiardi, G. Spoto, A. Zecchina, Phys. Chem. Chem. Phys. 7 (2005) 3948.
[56] M. Dinca, A.F. Yu, J.R. Long, J. Am. Chem. Soc. 128 (2006) 8904.
[57] M. Dinca, J.R. Long, J. Am. Chem. Soc. 129 (2007) 11172.
[58] J.L. Belof, A.C. Stern, M. Eddaoudi, B. Space, J. Am. Chem. Soc. 129 (2007) 15202.
[59] Y. Liu, H. Kabbour, C.M. Brown, D.A. Neumann, C.C. Ahn, Langmuir 24 (2008) 4772.